Biometals (2012) 25:1009–1022
DOI 10.1007/s10534-012-9567-1

Comparative analysis of stability and toxicity profile of three differently capped gold nanoparticles for biomedical usage

Sumistha Das · Nitai Debnath · Shouvik Mitra · Alokmay Datta · Arunava Goswami

Received: 11 April 2012 / Accepted: 15 June 2012 / Published online: 3 July 2012
© Springer Science+Business Media, LLC. 2012

Abstract Nowadays gold nanoparticle (GNP) is increasingly being used in drug delivery and diagnostics. Here we have reported a comparative analysis of detailed stability and toxicity (in vitro and in vivo) profile of three water soluble spherical GNPs, having nearly similar size, but the surfaces of which were modified with three different capping materials aspartic acid (GNPA), trisodium citrate dihydrate (GNPC) or bovine serum albumin (GNPB). Spectral analyses on the stability of these GNPs revealed that depending on the nature of capping agents, GNPs behave differently at different environmental modalities like wide range of pH, high salt concentrations, or in solutions and buffers of biological usage. GNPB was found to be extremely stable, where capped protein molecule successfully maintained its secondary structure and helicity on the nanoparticle, whereas colloidal stability of GNPA was most susceptible to altered conditions. In vitro cytotoxicity of these nanoparticle formulations in vitro were determined by water soluble tetrazolium and lactate dehydrogenase assay in human fibroblast cell line (MRC-5) and acute oral toxicity was performed in murine model system. All the GNPs were non-toxic to MRC-5 cells. GNPC had slight hepatotoxic and nephrotoxic responses. Hepatotoxicity was also evident for GNPA treatment. Present study established that there is a correlation between capping material and stability together with toxicity of nanoparticles. GNPB was found to be most biocompatible among the three GNPs tested.

Keywords Gold nanoparticles · Surface plasmon resonance · Stability · Cytotoxicity · Acute oral toxicity

Introduction

Metal nanoparticles (NP) are of immense interest to life science due to their successful applications in a multitude of biochemical and biophysical processes (Jain et al. 2008). Gold nanoparticle (GNP) is, in particular, the most popular because of the broad chemical versatility (Newman and Blanchard 2007) coming from its small size and non-specificity in its interactions and also because GNPs of accurate size and shapes can be synthesized by simple wet chemical method (Daniel et al. 2004) assuring reproducibility. They are easy to characterize due to collective oscillation of their outer shell electrons in the

Electronic supplementary material The online version of this article (doi:10.1007/s10534-012-9567-1) contains supplementary material, which is available to authorized users.

S. Das (✉) · N. Debnath · S. Mitra · A. Goswami
Biological Sciences Division, Indian Statistical Institute, 203 B.T. Road, Kolkata 700 108, West Bengal, India
e-mail: sumistha.das@gmail.com

A. Datta
Applied Material Science Division, Saha Institute of Nuclear Physics, Sector 1, Block-AF, Bidhannagar, Kolkata 700 064, West Bengal, India

conductance band at a frequency usually in the visible region of spectrum, giving rise to a strong Surface Plasmon Resonance (SPR) absorption (Eustis and El-Sayed 2006), and surfaces of these particles can easily be modified or capped with molecules containing thiol or amine functional groups (Sainsbury et al. 2007), imparting specificity in a controlled manner. Hence GNPs are widely used as nano-platforms for effective and targeted delivery of drugs overcoming many biological, biophysical, and biomedical barriers.

Drinking colloidal gold as panacea for different diseases, e.g. arthritis is an age old tradition (Swanson et al. 1949). Gold based anti-inflammatory agents like Auranofin® and Tauredon® have been widely used as a remedial for rheumatoid arthritis (Finkelstein et al. 1976). Recent studies on irradiation with focused laser pulses of suitable wavelength showed that GNPs can kill cancer cells (Loo et al. 2005; Huang et al. 2006; Chen et al. 2007). Moreover, GNP based drug carriers (Han et al. 2007) and intravenous contrast enhancers in medical imaging (Murray and Barnes 2007; McMahon et al. 2008) are also being extensively researched.

In spite of considerable progress in the field of synthesis, characterization, identification and biomedical application of GNPs, stability of these particles in high ionic strength and physiological conditions remains unclear and this becomes imperative if these NPs are to be utilized for medication. Again, Lewinski et al. 2008 have dealt with the interaction between different types of NPs and cells with respect to their size, shape and surface properties. However, GNPs with different capping may behave in different ways at cellular level by interacting with cell membrane, mitochondria, or nucleus and can impart adverse effects like organelle/DNA damage, mutagenesis, protein up/down regulation (Unfried et al. 2007; Aillon et al. 2009). Thus in vitro and in vivo toxicity studies of these NPs are necessary if these are to be employed in clinical applications, as different capping may affect the NP toxicity. In particular, no clear correlations have been established between the different capping of GNPs and the NP stability on one hand and toxicity on the other and we present here the first step towards these correlations. It is known that aggregation, agglomeration, precipitation and decomposition lead to distinctive changes in the SPR spectra of metal NPs. Hence we have used SPR spectroscopy as a reliable method to assess stability of GNPs with three organic capping under a range of environmental factors. Cytotoxicity assay of these NPs in vitro was determined by WST (Water Soluble Tetrazolium) assay and LDH (Lactate Dehydrogenase) assay in human fibroblast cell line (MRC-5). We have also shown detailed evaluation of acute oral toxicity study of GNPs in murine model system. Our in vivo toxicity study included general heath indicators such as behavioral abnormality, weight loss as well as specific tissue level toxicological studies including hematological toxicity, hepatotoxicity, nephrotoxicity etc. and microscopic assessment of morphological parameters of different organs of NP treated mice.

Materials and methods

Chemicals

Chemicals such as chloroauric acid, trisodium citrate dihydrate, DL-aspartic acid were purchased from Merck, Germany. HEPES (4-(2-hydroxyethyl)-1-piperazineethanesulfonic acid), sodium chloride, potassium chloride, disodium hydrogen phosphate, potassium dihydrogen phosphate, sodium pyruvate, non-essential amino acid, Ethylenediaminetetraacetic acid (EDTA) were procured from Sigma Aldrich, US. Dulbecco's modified Eagle's medium (DMEM), glutamine, streptomycin, penicillin were purchased from Himedia, India. Bovine serum albumin (BSA) was purchased from Calbiochem, India and fetal calf serum (FCS) was procured from Gibco, US. WST-1 assay kit (K302-500) and LDH assay kit (1008882) were purchased from BioVision, US and Cayman chemical, US respectively. Deionized water employed for the preparation of the solutions was obtained from a Sartorius Stedim (Germany) deionization system.

Synthesis of nanoparticle

Synthesis of aspartic acid capped (GNPA) and trisodium citrate dihydrate capped (GNPC) nanoparticle was based on simple wet chemical reduction of chloroaurate ions with minor modification of the standard protocol (Mandal et al. 2002; Turkevich et al. 1951). Aspartic acid/tri sodium citrate dihydrate was used as both reducing and stabilizing agent. For bovine serum albumin (BSA) capped GNP (GNPB), 90 ml of 3×10^{-4} M chloroaurate solution was prepared as solution I. 3.6 ml of 1 % trisodium citrate dihydrate

solution was prepared as solution II. Solution I and II were separately warmed to 60 °C and then solution II was drop wise added to solution I under continuous stirring. The resulting solution was stirred and heated up to 95 °C and cooled immediately after appearance of wine red coloration. The colloidal suspension was stored in refrigerator at 4 °C. BSA was dissolved in distilled water at 100 μg/ml concentration. Under continuous stirring mode, BSA solution was added drop wise to ice cold colloidal gold solution and stirring was continued until the solution became visibly clear.

Characterization of GNPs

The reduction of gold chloride and the formation of GNPs were detected spectroscopically. This was done by monitoring the SPR in terms of absorption spectra centered at ~520 nm using a UV–visible spectrometer (Perkin Elmer Lamda 25). Transmission electron microscopic (TEM) studies were employed for determination of size and morphology of GNPs. For this, a drop from colloidal dispersion of each sample was placed on a carbon coated copper grid and air dried to evaporate the solvent. Such prepared samples were observed under TEM (Techani, FEI Ltd.) in the bright field mode with an accelerating voltage at 80 kV. Size distribution of different surface functionalized GNPs was obtained by measuring the diameter of 200 particles viewed in the micrographs.

Stability study of GNPs

SPR patterns of three so synthesized GNPs in different pH domains were analyzed spectroscopically. Their stability in various ionic strengths and buffer solutions was also evaluated similarly. Different biological media including HEPES, NaCl (sodium chloride), and PBS (phosphate buffer saline) solutions were employed in different concentrations. 1 ml of each solution was added respectively to glass vials containing 1 ml of GNP solution and incubated for 24 h. To evaluate the constancy of different surface modifier on NP surface at physiological conditions (in vitro), GNPs were incubated in PBS containing 10 % FBS (fetal bovine serum) at 37 °C for 1 h. Thereafter, spectroscopic nature of these samples was analyzed.

In vitro cytotoxicity assay

The human fibroblast cells (MRC-5, purchased from American Type culture Collection) were maintained in continuous culture at 37 °C with 5 % CO_2 in DMEM containing 10 % heat-inactivated FCS, 2 mmol/L glutamine, 1 mmol/L sodium pyruvate, 100 U non-essential amino acid, 100 IU/ml penicillin, 100 μg/ml streptomycin. Toxicity of GNPs was studied using 2.0×10^4 cells placed in each well of a 96-well plate. 20 μl suspensions of GNPs in pH 7.0 phosphate buffer saline (PBS) were added to the cells for incubation. Final concentration of GNPs was 51, 128, 320, 800, 2,000 and 5,000 ppm. In negative control wells no treatment was given, only PBS was mixed with cell culture medium. The positive control cells were treated with EDTA, which would kill all the cells. WST-1 and LDH assays were carried out after the cells were incubated with GNPs for 72 h.

Viability of MRC-5 cells after GNP treatment was assessed in triplicate by WST-1 (Water Soluble Tetrazolium-1) assay with proper controls. In this study 10 μl of reconstituted WST-1 mixture was added to each well of a 96-well plate. The cells were incubated for 4 h at 37 °C in a CO_2 incubator. Before reading the absorbance, the plates were kept on an orbital shaker for one minute for gentle, homogeneous mixing of the color. The absorbance of the treated and untreated cells was measured using a micro titer plate reader at 450 nm.

The extent of cytotoxicity of SNPs on MRC-5 cells was estimated in triplicate in 96-well plate by measurement of LDH released from damaged cells into the medium using LDH assay kit. In brief, cell culture plates were centrifuged at 400 × g for 5 min. 100 μl of supernatant from each well of treated and a control cell was transferred to corresponding wells in a new 96-well plate. 100 μl of reconstituted reaction mixture was added to each well using multi channel pipetman. The plate was incubated at room temperature with gentle shaking on an orbital shaker for 30 min. The absorbance was taken at 490 nm in a microtiter plate reader. In this assay data were expressed as percentage of cytotoxicity in control and treated wells.

Acute oral toxicity of GNPs in mice

Healthy young nulliparous, non pregnant female mice and healthy young male mice (average body weight: 20 g) were kept in an animal house with controlled

temperature (23 °C ± 2 °C), humidity (60 % ± 10 %) and 12 h light/dark cycle. The mice were fed with standard rodent diet and filtered water. After 7 days of acclimatization the mice were randomly assigned to control and treatment groups. There were 5 mice of each sex in each group. 0.5 ml of GNP suspension was fed orally to the mice followed by feeding of this same volume after 12 h. Each mouse of the control group was fed with 1 ml deionised water in two doses of 0.5 ml each within an interval of 12 h.

The animals were kept under close observation for 14 days. Skin and fur changes, eye secretion and behavior patterns were observed. Special attention was paid to the clinical signs of toxicity including tremors, convulsions, salivation, nausea, vomiting, diarrhea, lethargy etc. At the end of 14 days they were sacrificed. Blood and serum from control and treated mice were analyzed for TC (total count), DC (differential count), Plt (platelet count), LDH (lactate dehydrogenase), creatinine, ALP (alkaline phosphatase), TP (total protein), cholesterol, TG (triglyceride), uric acid, BUN (blood urea nitrogen), SGOT (serum glutamic oxaloacetic transaminase), SGPT (serum glutamic pyruvic transaminase) and phosphorous level. Heart, lungs, liver, kidney, spleen, uterus and testis were carefully removed and fixed in 10 % formalin solution containing neutral phosphate buffer saline. Thereafter the organs were embedded in paraffin, sectioned at 5 μm, mounted on glass slide and stained with eosin–hematoxylin using standard histopathological techniques. Sections were examined under light microscope. The animals were weighed before and after the completion of the experiment.

All the experiments were performed following OECD guideline 420 (OECD 2001).

Statistical analysis

Values are presented as the mean ± standard error of the mean. The statistical significance was evaluated by one-way analysis of variance followed by students-'*t*' test at 5 % level of significance between controls ($P < 0.05$) using R 2.14.2 software.

Results

GNPs synthesized are almost monodisperse and had nearly equal size and shape. Figure 1a–c show a representative TEM image recorded from colloidal solutions of GNPA, GNPC and GNPB respectively. GNPs synthesized are uniform in size which indicates that they are adequately protected by their respective capping materials in almost all cases. The average particle size range of GNPA, GNPC and GNPB was 15–20 nm. The size distribution of synthesized NPs is shown in supplementary material (Fig. S1).

Insets in Fig. 1 shows the UV–Vis spectra recorded from the colloidal gold solutions of different surface properties. In Fig. 1a–c a strong absorption at near about 521–527 nm was observed; this absorbance peak corresponds to GNP's free conduction electrons induced by an interacting electromagnetic field or localized SPR. A strong plasmon absorption peak at 521 nm (Fig. 1c inset-blue line) attributed to GNPs before BSA stabilization. The red line in Fig. 1c inset corresponds to UV–Vis absorption spectra of GNPs after stabilization with BSA. After modification with BSA the plasmon absorption peak of GNPs shifted from 521 to 524.91 nm. Temperature, refractive index of surrounding medium, size and shape of NPs are the factors involved in resonance wavelength and bandwidth of GNPS. Here changes of dielectric nature surrounding the GNP due to presence of BSA ($n = 1.9$) is the reason behind peak shift confirming the addition of BSA molecule to GNP.

The stability of GNPs depends on their surface capping agents

Figure 2 shows the result of stability study of gold colloid at different pH conditions. In case of GNPA (Fig. 2a), SPR band remained stable except at extreme acidic pH conditions. At pH level 1, the characteristic SPR peak was shifted to 537 nm from 527 nm and an extra peak at 649.80 nm was observed. From this it can be concluded that GNPA remained stable except extreme acidic pH domain. In case of GNPC (Fig. 2b) similar trend of result was found. Here at extreme acidic and basic condition the normal SPR peak at 527 nm was shifted to 537.93 and 586 nm respectively. GNPB was comparatively more stable in both acidic and alkaline pH domain (Fig. 2c).

Stability of these GNPs was also studied in a variety of molecules of biological interest like PBS, HEPES and NaCl. Normal saline or 0.154 M NaCl solution is commonly used as intravenous dips for patients with danger of developing dehydration or hypervolemia. So

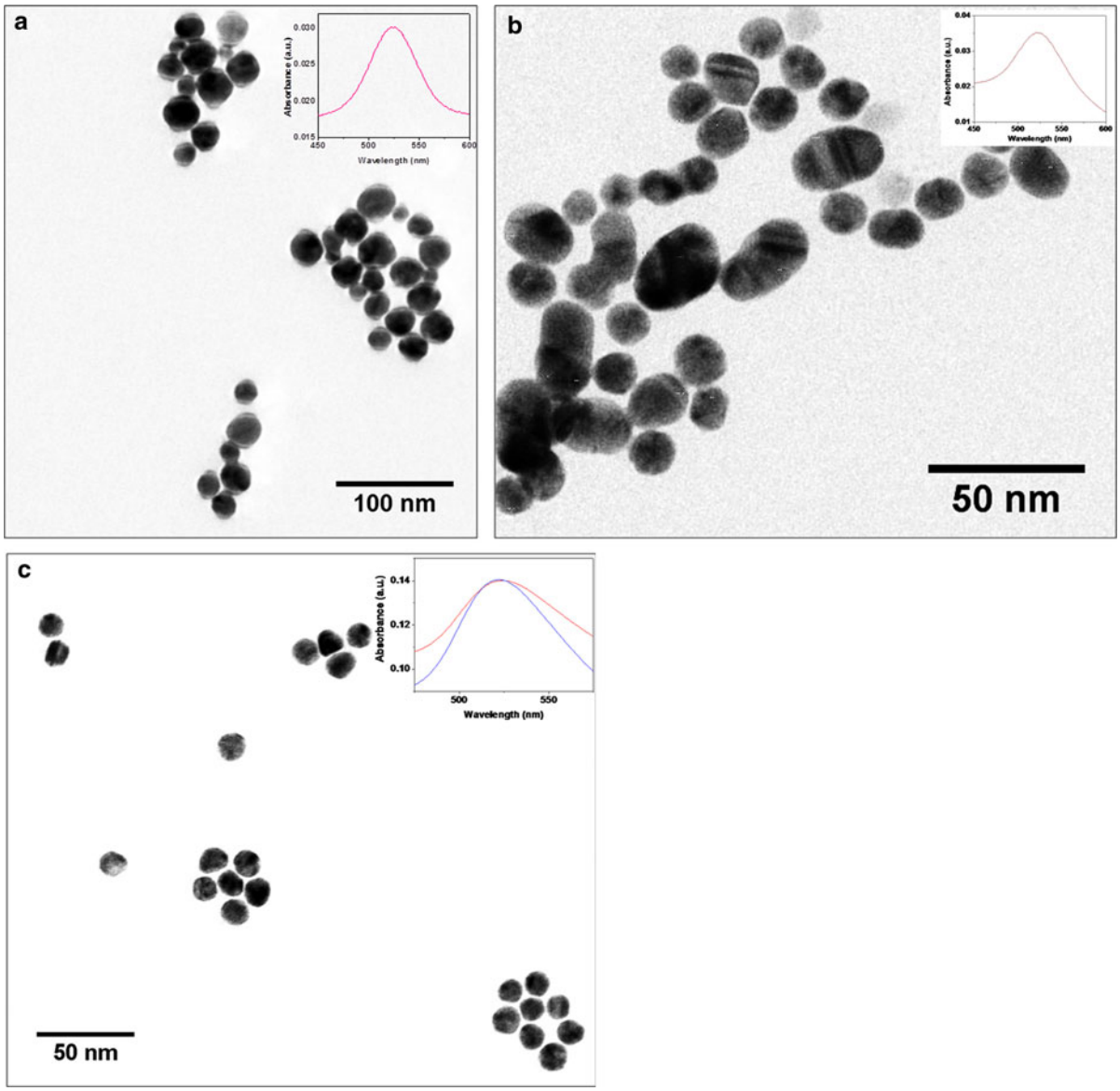

Fig. 1 TEM image of **a** GNPA **b** GNPC and **c** GNPB. *Inset* of **a** and **b** show the representative absorption spectra of GNPA and GNPC respectively. *Inset* of **c**: absorption spectra before (*blue line*) and after (*red line*) BSA stabilization. (Color figure online)

GNPA, GNPB and GNPC were incubated in 0.08, 0.154 and 0.31 M NaCl solution for 24 h and their stability was evaluated by measuring the characteristic SPR spectra. PBS, a commonly used buffer solution, is isotonic and non-toxic to cells and thus has wide biomedical application. HEPES is an organic zwitterionic buffer, where the secondary and tertiary amine groups provide positive charge, whereas sulphonic and carboxylic acid groups are responsible for negative charges. It is widely used to maintain pH levels of basal media in cell culture.

Figure 3a represents the SPR pattern of GNPA in presence and absence of aforementioned biologically relevant molecules. Amongst three GNPs, GNPA was most prone to agglomeration. At lowest concentration of NaCl characteristic SPR spectra of GNPA shifted widely to 544 nm, associated with peak broadening. Immediately after addition of 0.31 M NaCl, GNPA

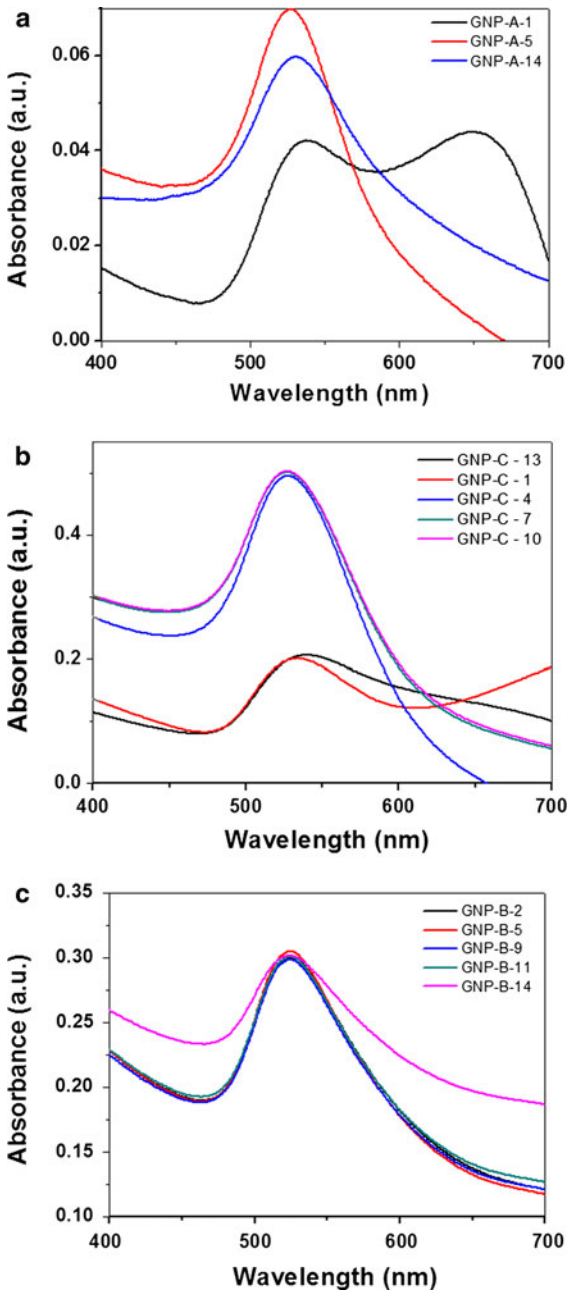

Fig. 2 UV-vis spectra of **a** GNPA **b** GNPC and **c** GNPB solutions recorded at 24 h with different pH value

suspension lost its usual red color to become light blue and characteristic SPR peak completely disappeared, indicating agglomeration and precipitation of NPs. Again it lost its characteristic color and SPR pattern in presence of PBS at or beyond 50 mM concentration. In case of HEPES, no significant shift in the UV–Vis absorption spectra was noticed within 24 h of observation, indicating the stability of these particles in all concentrations of HEPES solutions considered.

Figure 3b shows the stability profile of GNPC. Agglomeration and precipitation of GNPC were observed when NaCl and PBS strength reached to

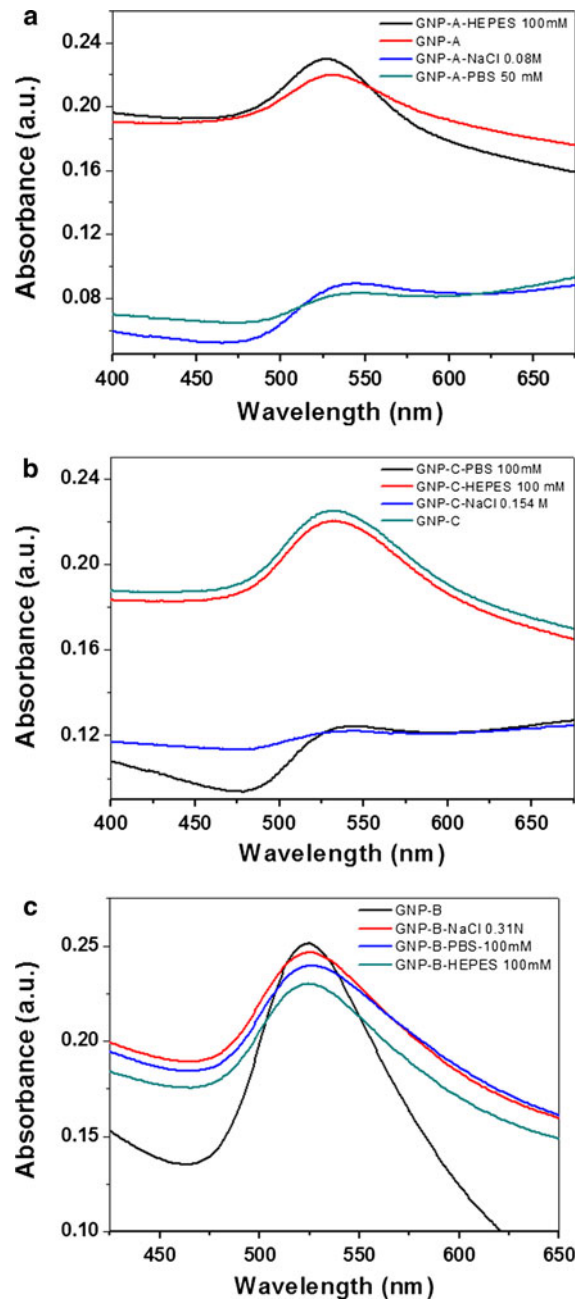

Fig. 3 UV-vis spectra of **a** GNPA **b** GNPC and **c** GNPB solutions recorded at 24 h with different additives

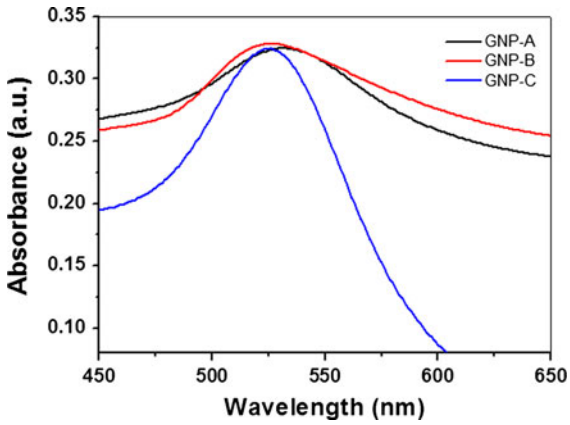

Fig. 4 UV-vis spectra of citrate–stabilized, aspartate-stabilized and BSA-stabilized GNP solutions recorded at 24 h with FBS

0.154 M and 100 mM respectively. Like GNPA, GNPC was also found to be stable in HEPES solution.

Spectral pattern of GNPB, when observed at different strengths of NaCl, PBS and HEPES solutions is presented in Fig. 3c. Any significant change in SPR pattern was not apparent in any case which indicates that GNPB was most stable among the three GNPs evaluated.

FBS is a supplement for a number of macromolecular proteins, low molecular weight nutrients, carrier proteins for water insoluble components in basal growth media required for in vitro growth of cells. FBS was engaged in our study to evaluate the stability of aforementioned NPs in physiological conditions before their application to cell culture medium. Figure 4 represents the FBS stability profile of three GNPS. All of them were fairly stable in presence of FBS without sign of any significant SPR peak shift.

In vitro toxicity revealed all the GNPs to be non-cytotoxic

The effect GNPA, GNPB and GNPC in human fibroblast cell line (MRC-5) was examined in terms of their effect on cell proliferation by the WST-1 assay. In WST-1 assay tetrazolium salt (4-[3-(4-iodophenyl)-2-(4-nitrophenyl)-2H-5-tetrazolio]-1, 3-benzene disulfonate) is cleaved to formazan (produce purple colored crystals) by mitochondrial dehydrogenase enzyme from live cells and its absorption can be measured spectroscopically. Hence, the increase in formazan dye is directly correlated to the number of metabolically active living cells. The cell survival rates were determined against the negative control (Fig. 5). The cell survival rate decreased negligibly with increasing concentration of GNPs. At 51 ppm 93, 98 and 91 % cells were viable with GNPA, GNPB and GNPC treatment. 76, 77 and 70 % cells were alive even after administration of 5,000 ppm GNP A, GNPB and GNP C treatments respectively. But LD_{50} was not achieved in any case even after administration of 5,000 ppm dosage.

The cytotoxicity of GNPs was further evaluated by LDH assay. Similar trend of result was also evident

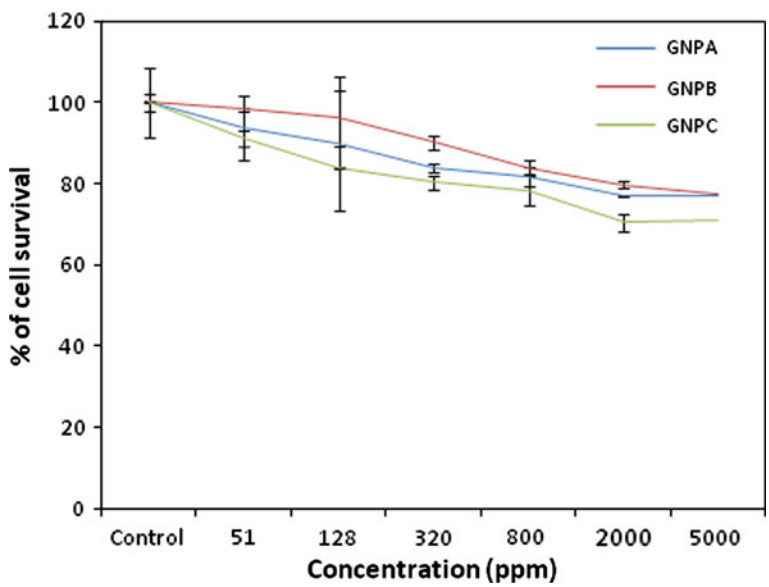

Fig. 5 Survivability of MRC-5 cells (±SE) after 72 h incubation with GNPs using WST-1 assay

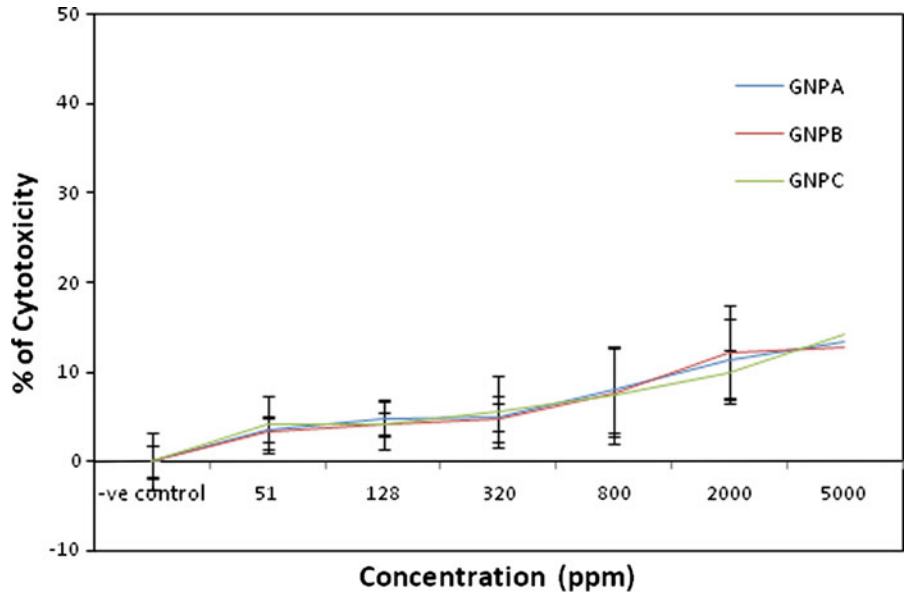

Fig. 6 Percentage of cytotoxicity of MRC-5 cells (±SE) after 72 h incubation with GNPs using LDH assay

from GNP induced toxicity profile obtained from LDH assay (Fig. 6). LDH, a soluble enzyme located in the cytoplasm of cells, is released into the surrounding culture medium when cells are damaged. LDH activity in the culture medium can therefore be used as an indicator of cell membrane integrity, and consequently as a measure of cytotoxicity. In the untreated cells, there was negligible amount of LDH present in the culture medium because most of the cells were intact. In EDTA treated cells presence of LDH was highest because almost all the cells died due to EDTA treatment and hence, the LDH present in culture medium was taken as 100 %. At 51 ppm GNPA and GNPB caused 3.57 and 3.27 % cytotoxicity respectively (Fig. 6), whereas 4.16 % toxicity was observed when GNPC was applied at this dosage. The cytotoxicity level of GNPA, GNPB and GNPC was 13.39, 12.8 and 14.28 % at 5,000 ppm respectively. CC50 (50 % cellular cytotoxicity) of the GNPs was not observed even at 5,000 ppm dosage.

Acute oral toxicity of GNPs in murine model system

In vivo toxicity studies of synthesized NPs are important and they will not only overcome the limitations of in vitro studies but also will open new avenues towards GNP based biomedical applications.

No mortality was evident throughout the experimental period. Treated group of mice exhibited normal and consistent gain of bodyweight with respect to the control mice (data not shown). Signs of behavioral abnormality were absent. Mice did not show any clinical symptoms of toxicity including tremors, convulsions, salivation, nausea, vomiting, diarrhea, lethargy, skin or fur color changes and loss of appetite.

Table 1 represents the comparative analysis of hematological parameters of GNP treated and control mice. Hemoglobin content was increased by GNPs. Elevated level of RBC concentration along with high hemoglobin count is associated with erythrocytosis and polycythemia. As RBC count was unaltered by any of the treatments, secondary increase in hemoglobin count may be associated with stress response. Amongst differential count parameters of blood, lymphocyte cell population was elevated by GNPC and GNPA treatment but remained unaltered in GNPB treatment. Platelet count and erythrocyte sedimentation rate was found to be consistent with control group of mice.

Metabolic enzymes such as ALP, SGOT and SGPT are responsible for putative functioning of liver and any abnormality induced may lead to excessive leakage of these enzymes in the blood stream. Thus the effect of GNPs on the level of these metabolic

Table 1 Hematological analysis of control and GNP treated mice

Parameters	Control	GNPA	GNPB	GNPC
Hemoglobin	13.5 ± 0.45	16.1 ± 0.6*	15.6 ± 0.7*	15.7 ± 1.2*
TC				
RBC ($\times 10^6$ mm^{-3})	4.1 ± 0.4	4.6 ± 0.7	4.3 ± 0.3	5.1 ± 0.2
WBC ($\times 10^2$ mm^{-3})	56 ± 0.07	58 ± 0.17	56.8 ± 0.11	57.3 ± 0.4
DC (%)				
Neutrophils	42 ± 3	43 ± 4	44 ± 1	42 ± 1
Lymphocytes	53 ± 1	64 ± 4*	52 ± 3	66 ± 3*
Monocytes	2	2	2	2
Eosinophils	3 ± 0.57	2	3 ± 0.57	2
Basophils	0	0	0	0
Platelets ($\times 10^5$ mm^{-3})	1.54 ± 0.04	1.56 ± 0.03	1.52 ± 0.03	1.6 ± 0.02
ESR (1 h)	12 ± 1	10 ± 1	12 ± 2	12 ± 2
ESR (2 h)	16 ± 3	16 ± 5	16 ± 1	15 ± 1

* Significant difference versus control, $P < 0.05$

enzymes shaping the appropriate functioning of liver through serum analysis was evaluated. Treatment with GNPC significantly increased serum SGOT and SGPT level indicating abnormal functioning of liver. Similarly, SGOT level was also elevated by GNPA treatment. In contrast, GNPB treated mice did not show any disruptive change to liver health (Table 2). Parameters such as creatinine, BUN and uric acid are blood metabolites correlated to kidney health. The level of creatinine symptomatic of altered glomerular filtration rate was also significantly turned up by GNPC treatment (Table 3). Similar trend was evident for BUN. GNPA and GNPB treated mice did not show any significant changes in renal heath parameters when compared to control.

Various parameters of blood lipid profile were tested in control and treated mice. High blood cholesterol and triglyceride levels are directly implicated in increased chances of developing coronary heart diseases and atherosclerosis (hardening of arteries) respectively. The study over the serum lipid profile revealed that exposure of GNPs in aforementioned dosages did not alter lipid content (supplementary material: Table S1). Various factors like bone metastasis, hypocalcemia, sarcoidosis, hyperparathyroidism etc. causes abnormal level of phosphorus in blood. Total protein estimation measures nutritional status and helps to diagnose different kidney or liver related diseases. None of the GNPs conferred any deleterious change in phosphorus and total protein content (supplementary material: Table S2).

Histopathological studies are well established experiments for toxicity dependent morphological alteration analysis. Toxicity profile of NP has considerable

Table 2 Effect of GNPs over the metabolic enzymes (Liver)

Parameters	Control	GNPA	GNPB	GNPC
Alkaline phosphatase (U/L)	60 ± 2	62 ± 2	61 ± 4	59 ± 2
SGOT (U/L)	12 ± 2	19 ± 2*	11 ± 1	21 ± 3*
SGPT (U/L)	11 ± 10	14 ± 5	13 ± 1	22 ± 7*

* Significant difference versus control, $P < 0.05$

Table 3 Effect of GNPs over kidney parameters

Parameters	Control	GNPA	GNPB	GNPC
Creatinine (mg/dl)	0.71 ± 0.03	0.76 ± 0.08	0.72 ± 0.02	0.89 ± 0.06*
Uric acid (mg/dl)	2.9 ± 0.1	2.6 ± 0.6	3.0 ± 0.1	3.1 ± 0.1
BUN (mg/dl)	10 ± 2	12 ± 1	11 ± 2	16 ± 3*

* Significant difference versus control, $P < 0.05$

relation with alteration in tissue and cell morphology of a scale that can be visualized under light microscope (Reeves et al. 2010). Pathological effect of our nanostructures on morphological features of different organs from control and treated mice was studied microscopically using hematoxylin-eosin stained sections of the organs.

Histology of liver demonstrated normal morphometry of hepatocytes and hepatic portal triad in control mice (Fig. 7a). GNPB did not show any deleterious damage to liver histology (Fig. 7b). But liver health was perturbed by GNPA and GNPC treatment (Fig. 8). Primary alterations evident for liver tissue damage were hepatocytic disarray, infiltration of inflammatory cells in portal triad, dilation of the sinusoids, fatty degeneration locally affecting the liver lobule, and widely dilated and congested central vein compared to tissues obtained from control mice. The

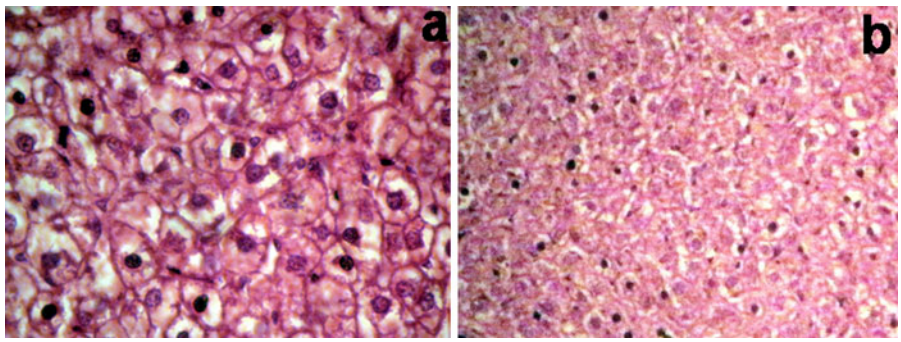

Fig. 7 Photomicrographs of liver. The pictures **a** and **b** represented the livers from control and GNPB treated mice respectively. No abnormal morphology was observed in the two groups

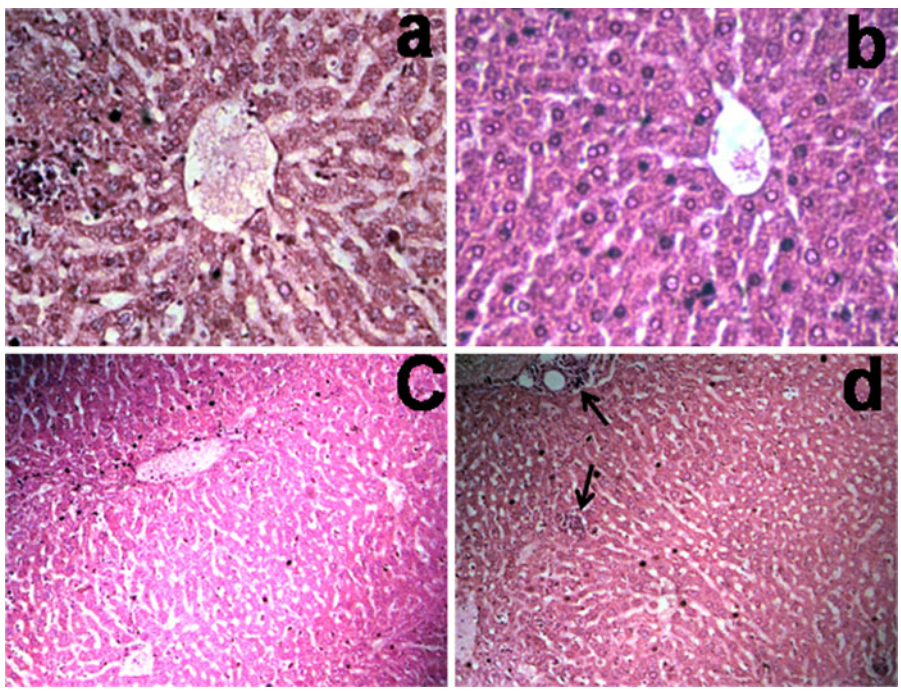

Fig. 8 GNPC and GNPA exposure altered histopathological architecture of the liver **a** GNPA treatment showed widely dilated and congested central vein, sinusoidal dilation and hepatocytic disarray **b** GNPC treated mice demonstrating widely dilated congested central vein **c** Fatty degeneration focally affecting the liver lobules of GNPC group of mice **d** lobular infiltrate by chronic inflammatory cells in GNPC treated mice (*arrows*)

reason behind infiltration of inflammatory cells (lymphocytes and plasma cells) in treated mice liver may indicate enhanced defence mechanism against foreign particles. The sinusoids became prominent, widely dilated and congested when exposed to GNPA and GNPC. Sub acute hepatotoxicity was indicated by vacuolated swelling of the sinusoids and disarray of hepatocytes in treated mice. Fatty alteration was observed in some swollen hepatocytes due to lipid peroxidation that leads to rough endoplasmic damage and detachment of cytoplasmic lipoprotein with probable risk of irregular fat metabolism (Reddy et al. 2006).

Histology of renal tissue did not show any considerable alteration for control and GNPB treatment (Fig. 9). Some tubular alterations were observed in kidney tissue of GNPC treated mice (Fig. 10). Vacuolization of renal cells was observed in the renal tubules which might be a result of ion and fluid homeostasis leading to an increase of intracellular water (Schrand et al. 2010). Anisokaryosis or variable nuclei sizes were also observed in some renal cells. But on the contrary, GNPA and GNPB treatment did not show any sign of evident change from regular morphology of renal cortex and glomerular tuft.

The histopathological findings established that GNPs had no toxic effect on mice heart, lung, spleen and testis (supplementary material: Fig. S2). Histological section of GNP treated heart was showing normal appearing endocardium and striated cardiac fibers with regular branching. Similarly lung tissue of treated mice presented a normal appearance. Histological study of lung tissue from control mice showed normal alveolar pattern. Normal alveolar membranes and parenchymal blood vessels of lung tissues were also seen in treated group of mice. The study of the spleen histology of treated mice was also consistent with control group of mice. No sign of organ damage was found from histological sections of testes from treated male mice. Clear Sertoli cell, seminiferous tubule and epididymis with normal histology were evident from all sets of treated mice. Ovary section

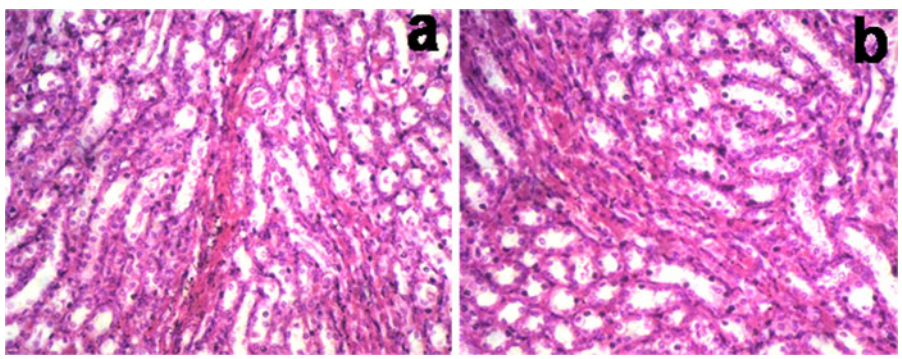

Fig. 9 Photomicrographs of kidney. Pictures **a** and **b** represented the kidneys from control and GNPB treated mice respectively. No abnormal morphology was observed in the two groups

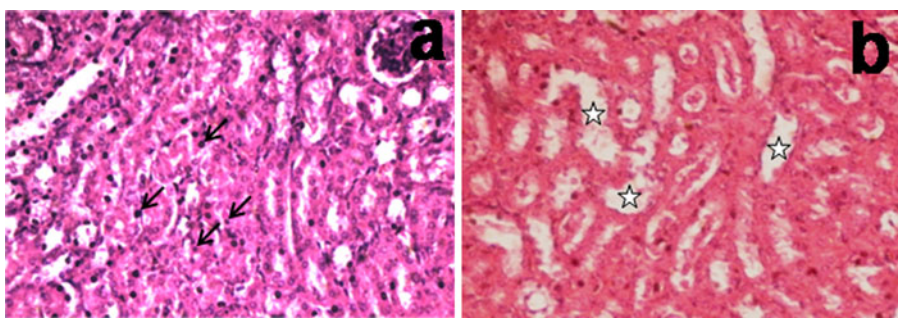

Fig. 10 Histopathological alteration of kidney after receiving GNPC. Pictures **a** demonstrating anisokaryosis (*arrows*) and **b** showing vacuolar degeneration (*stars*)

was also unaffected indicated from normal histology with distinct oocytes and primary follicles (data not shown). All the slides were also re-analyzed by an experienced pathologist. Examined reports obtained from him were also corroborated with our findings.

Discussion

Here we have presented detailed comparative analysis of stability and biocompatibility of three spherical GNPs having similar size but different surface capping materials. It was evident that surface capping played a vital role in maintaining stability of NPs in altered environmental conditions. GNPA was found to be most vulnerable to losing their surface capping functionality and was prone to agglomeration. GNPC was unstable in highest concentrations of NaCl and PBS solutions used. Since citrate and aspartate both contained acidic group, the surface carboxylic acid groups were protonated resulting their destabilization. With the increasing pH of the solution the surface carboxylic acid groups are deprotonated to $-CO_2^-$, hence stability is increased resulting higher dispersed nature of the particle as revealed from the SPR peak. However at extremely alkaline pH, GNP can undergo some sort of agglomeration which is again reflected in their shifted SPR peak. Meanwhile in case of GNPB, the long protein chain of BSA was able to maintain its normal helicity in all the experimental conditions, due to the absence of acidic carboxylic group.

Size dependent in vitro and in vivo toxic effect of GNP was reported by Chen et al. (2009) and Pan et al. (2007) respectively. Uboldi et al. (2009) reported that GNPC was toxic to alveolar type-II cell lines A549 and NCIH441. Though dose dependent cell mortality was evident from both WST-1 and LDH assays in our study, LD_{50} was not observed for any of the GNPs used even after administration of 5,000 ppm dosage. The cause of cell death with increasing doses of GNPs might be due to the interference of NPs with membrane function or metabolism. Non toxic effect of gold nanospheres of different size (4, 12, and 18 nm in diameter) and capping agents (citrate, cysteine, glucose, biotin, and cetyltrimethyl-ammonium-bromide) using a human leukemia cell line was also reported earlier (Connor et al. 2005).

From acute oral toxicity study in mice model, some pathological parameters were found to be altered by GNPs. Our serum biochemical data suggest that instillation of GNPC and GNPA may be associated with an elevation of alanine aminotransferases (SGOT and SGPT). Release of these liver enzymes to circulation is associated with hepatocytic damage (Turkez et al. 2010). In addition to the changes in the liver circulating enzymes GNPC also significantly elevated blood metabolites related to kidney health. Increased level of lymphocyte cell count is indication of elevated immune response to foreign material in GNPC and GNPA treated mice. Result from our histopathological studies is also consistent with liver biochemical parameters. Most prominent amongst liver histopathological abnormalities observed are dilation and congestion of central vein, sinusoidal dilation, infiltration of inflammatory cells etc. Dilation of central vein may be associated with turbulence of membrane function that leads to massive influx of water and Na^+. In addition, congestion of them might be the result of leakage of lysosomal hydrolytic enzymes that leads to cytoplasmic degeneration and macromolecular crowding (Del Monte et al. 2005). The appearance of inflammatory cells may indicate a sort of defense mechanism. Sinusoidal dilatation is the increased gap between the hepatic cords in the hepatic lobule and was observed in only GNPA treatment. We also noted sub acute renal injury caused by GNPC, indicated by appearance of vascular degeneration and anisokaryosis. This type of GNP induced hepatic and renal tissue alterations was also noticed by Abdelhalim and Jarrar (2011, 2012). Given our findings that GNPs, at least at the levels used in the present study, do not induce substantial damage to heart, lung, spleen, testis and ovary of mice. It is likely that the liver and kidney by acting to clear NPs from the circulation, is preventing additional secondary or tertiary pathological changes to other organs.

Conclusion

To the best of our knowledge this is the first report on detailed comparative analysis on the role of surface capping material on stability and toxicity (both in vitro and in vivo) of three water soluble GNPs of similar size and shape. From the present work there is a clear indication that these alterations in stability and toxicity by GNPs are dependent on surface functionalities. Aspartic acid was found to be least potent in maintaining GNP stability in different biologically

relevant molecules and buffers and was also found to be hepatotoxic. Citrate capping could confer moderate stability on GNP, but exhibited nephrotoxicity and hepatotoxicity. GNPB was found to be most suitable amongst all three GNPs tested for biomedical application. Further extensive pathological, histomorphological, histochemical and ultrastructural investigations are desirable to conclude a beneficial relationship between surface capping agent and GNPs for their successful biomedical application with respect to their potential use to therapeutic and diagnostic use in correlation with their size, chemical composition, solubility, surface charge and structure.

Acknowledgments Authors would like to thank Department of Biotechnology, Govt. of India (Grant Nos. BT/PR9050/NNT/28/21/2007, BT/PR15217/NNT/28/506/2011 and BT/BIPP 0439/11/10) and Indian Council of Agriculture Research (Grant Nos. NAIP/Comp-4/C3004/2008-09 and NFBSFARA/GB-2019/2011-12) for their financial support. Indian Statistical Institute (ISI) plan project for 2011–2012 was also used for funding this work. Authors are also grateful to Mrs. Indrani Roy for her valuable suggestions regarding this manuscript.

References

Abdelhalim MAK, Jarrar BM (2011) Renal tissue alterations were size-dependent with smaller ones induced more effects and related with time exposure of gold nanoparticles. Lipids in Health and Dis 10:163–168

Abdelhalim MAK, Jarrar BM (2012) Histological alterations in the liver of rats induced by different gold nanoparticle sizes, doses and exposure duration. J Nanobiotechnol 10:5–13

Aillon KL, Xie Y, El-Gendy N, Berkland CJ, Forrest ML (2009) Effects of nanomaterial physicochemical properties on in vivo toxicity. Adv Drug Deliv Rev 61:457–466

Chen J, Wang D, Xi J, Au J, Siekkinen A, Warsen A, Li ZY, Zhang H, Xia Y, Li X (2007) Immuno gold nanocages with tailored optical properties for targeted photothermal destruction of cancer cells. Nano Lett 7:1318–1322

Chen YS, Hung YC, Liau I, Huang GS (2009) Assessment of the in vivo toxicity of gold nanoparticles. Nanoscale Res Lett 4:858–864

Connor EE, Mwamuka J, Gole A, Murphy CJ, Wyatt MD (2005) Gold nanoparticles are taken up by human cells but do not cause acute cytotoxicity. Small 1:325–327

Daniel MC, Astruc D (2004) Gold nanoparticles: assembly, supramolecular chemistry, quantum-size-related properties, and applications toward biology, catalysis, and nanotechnology. Chem Rev 104:293–346

Del Monte U (2005) Swelling of hepatocytes injured by oxidative stress suggests pathological changes related to macromolecular crowding. Med Hypotheses 64:818–825

Eustis S, El-Sayed MA (2006) Why gold nanoparticles are more precious than pretty gold: noble metal surface plasmon resonance and its enhancement of the radiative and nonradiative properties of nanocrystals of different shapes. Chem Soc Rev 35:209–217

Finkelstein AE, Walz DT, Batista V, Mizraji M, Roisman F, Misher A (1976) Auranofin. New oral gold compound for treatment of rheumatoid arthritis. Ann Rheum Dis 35: 251–257

Han G, Ghosh P, Rotello VM (2007) Functionalized gold nanoparticles for drug delivery. Nanomedicine 2:113–123

Huang X, El-Sayed IH, Qian W, El-Sayed MA (2006) Cancer cell imaging and photothermal therapy in the near-infrared region by using gold nanorods. J Am Chem Soc 128: 2115–2120

Jain PK, Huang X, El-Sayed IH, El-Sayed MA (2008) Noble metals on the nanoscale: optical and photothermal properties and some applications in imaging, sensing, biology, and medicine. Acc Chem Res 41(12):1578–1586

Lewinski N, Colvin V, Drezek R (2008) Cytotoxicity of nanoparticles. Small 4:26–49

Loo C, Lowery A, Halas N, West J, Drezek R (2005) Immunotargeted nanoshells for integrated cancer imaging and therapy. Nano Lett 5:709–711

Mandal S, Selvakanan PR, Phadtare S, Pasricha R, Sastry M (2002) Synthesis of a stable gold hydrosol by the reduction of chloroaurate ions by the amino acid, aspartic acid. Indian Acad Sci (Chem Sci) 114:513–520

McMahon SJ, Mendenhall MH, Jain S, Currell F (2008) Radiotherapy in the presence of contrast agents: a general figure of merit and its application to gold nanoparticles. Phys Med Biol 53:5635–5651

Murray WA, Barnes WL (2007) Plasmonic Materials. Adv Mater 19:3771–3782

Newman JDS, Blanchard GJ (2007) Formation and encapsulation of gold nanoparticles using a polymeric amine reducing agent. J Nanopart Res 9:861–868

Organization for Economic Cooperation and Development (OECD) (2001) OECD guidelines for testing of chemicals. Test guideline 420. Acute Oral toxicity—fixed dose procedure, OECD, Paris

Pan Y, Neuss S, Leifert A, Fischler M, Wen F, Simon U, Schmid G, Brandau W, Jahnen-Dechent W (2007) Size-dependent cytotoxicity of gold nanoparticles. Small 3:1941–1949

Reddy JK, Rao MS (2006) Lipid metabolism and liver inflammation. II. Fatty liver disease and fatty acid oxidation. Am J Physiol Gastrointest Liver Physiol 290:G852–G858

Reeves CL, Romero DG, Barria MA, Olmedo I, Clos A, Ramanujam VMS, Urayama A, Vergara L, Kogan MJ, Soto C (2010) Bioaccumulation and toxicity of gold nanoparticles after repeated administration in mice. Biochem Biophys Res Commun 393:649–655

Sainsbury T, Ikuno T, Okawa D, Pacilé D, Fréchet JMJ, Zettl A (2007) Self-assembly of gold nanoparticles at the surface of amine- and thiol-functionalized boron nitride nanotubes. J Phys Chem C 111:12992–12999

Schrand AM, Rahman MF, Hussain SM, Schlager JJ, David A, Smith DA, Syed AF (2010) Metal-based nanoparticles and their toxicity assessment. Nanomed Nanobiotechnol 2: 544–568

Swanson JN (1949) The value of repeated colloidal gold tests in rheumatoid arthritis. Ann Rheum Dis 8:232–237

Turkevich J, Stevenson PC, Hillier J (1951) A study of the nucleation and growth processes in the synthesis of colloidal gold. Faraday Soc 11:55–75

Turkez H, Yousef MI, Geyikoglu F (2010) Propolis prevents aluminium-induced genetic and hepatic damages in rat liver. Food Chem Toxicol 48:2741–2746

Uboldi C, Bonacchi D, Lorenzi G, Hermanns MI, Pohl C, Baldi G, Unger RE, Kirkpatrick CJ (2009) Gold nanoparticles induce cytotoxicity in the alveolar type-II cell lines A549 and NCIH441. Part Fibre Toxicol 6:18–29

Unfried K, Albrecht C, Klotz L, Mikecz AV, Grether-Beck S, Schins RPF (2007) Cellular responses to nanoparticles: target structures and mechanisms. Nanotoxicology 1: 52–71